

miniaturization of the filters irrespective of dielectric constant of the substrates. The filters of the Refs. 4, 5, 6, and 8 are the most compact dualband filters published up to the date. The filter of Ref. 4 is compact in size and has extended upper stopband above 7 GHz, but has poor selectivity, low attenuation in lower and middle stopbands. The miniature dualband filter of the Ref. 5 has wide upper stopband above 9 GHz for the second passband frequency of 5.7 GHz; however the attenuation in middle stopband is only 20 dB due to the coupling between closely spaced components. The upper stopband of the filters of the Refs. 6, 8 are limited to 9 GHz and 7 GHz, respectively. The filters presented here are compact in size along with wide and deep upper stopband as well as a deep mid-stopband.

4. CONCLUSION

The design and implementation of the compact dualband bandpass filters with deep and wide stopbands using anti-parallel coupled folded SIR and open stub have been presented. Dualband filters with different second passband frequencies at 2.45/5.25 GHz and 2.45/5.75 GHz are realized using two different folded architectures. The wide and deep upper stopband is achieved by suppressing spurious response of the filter using open stub. Also, the attenuation in stopband is deep and sharp.

ACKNOWLEDGMENTS

This work was supported in part by the National Science Council of Taiwan under the contract NSC95-2221-E-006-428-MY3, the Ministry of Education Program for Promoting Academic Excellence of Universities under the Grant A-91E-FA08-1-4, and the Foundation of Chen, Jieh-Chen Scholarship of Tainan, Taiwan.

REFERENCES

1. C.-Y. Chen and C.-Y. Hsu, A simple and effective method for microstrip dual-band filters design, *IEEE Microwave Wireless Compon Lett* 16 (2006), 246–248.
2. M.-I. Lai and S.-K. Jeng, Compact microstrip dual-band bandpass filters design using genetic-algorithm techniques, *IEEE Trans Microwave Theory Tech* 54 (2006), 160–168.
3. S. Sun and L. Zhu, Compact dual-band microstrip bandpass filter without external feed, *IEEE Microwave Wireless Compon Lett* 15 (2005), 644–646.
4. J. Wang, Y.-X. Guo, B.-Z. Wang, L. C. Ong, and S. Xiao, Compact and low loss dualband bandpass filter using pseudo-interdigital stepped impedance resonators for WLANs, *IEEE Microwave Wireless Compon Lett* 17 (2007), 187–189.
5. C.-Y. Chen, C.-Y. Hsu, and H.-R. Chuang, Design of miniature planar dualband filter using dual-feeding structures and embedded resonators, *IEEE Microwave Wireless Compon Lett* 16 (2006), 669–671.
6. H.-K. Jhuang, C.-H. Lee, and C.-I. G. Hsu, Design of compact microstrip dual band bandpass filters with $\lambda/4$ stepped-impedance resonators, *Microwave Opt Technol Lett* 49 (2007), 164–168.
7. S. Sun and L. Zhu, Novel design of dualband microstrip bandpass filters with good in-between isolation, *Proceedings of Asia Pacific Microwave Conference*, Suzhou, China, 2005, pp. 1–4.
8. P.K. Singh, S. Basu, and Y.-H. Wang, Miniature dualband filter using quarter wavelength stepped impedance resonators, *IEEE Microwave Wireless Compon Lett* 18 (2008), 88–90.

© 2009 Wiley Periodicals, Inc.

VERY-SMALL-SIZE FOLDED LOOP ANTENNA WITH A BAND-STOP MATCHING CIRCUIT FOR WWAN OPERATION IN THE MOBILE PHONE

Yun-Wen Chi and Kin-Lu Wong

Department of Electrical Engineering National Sun Yat-Sen University Kaohsiung 80424, Taiwan; Corresponding author: chiyw@ema.ee.nsysu.edu.tw

Received 8 July 2008

ABSTRACT: A folded loop antenna with a band-stop matching circuit for wireless wide area network (WWAN) operation in the mobile phone is presented. The folded loop antenna alone occupies a very small volume of 0.6 cm^3 only, yet it can generate a lower band covering GSM850 operation and an upper band covering GSM1800/1900/UMTS operation. By incorporating a band-stop matching circuit with a central frequency at about 1.05 GHz and a 3-dB band-stop bandwidth of less than 200 MHz, the antenna's lower band can have a dual-resonance behavior, hence resulting in a much widened operating band capable of covering GSM850/900 operation. In addition, such a band-stop matching circuit shows very small effects on the antenna's upper band. This property makes it easy for the antenna to cover GSM850/900/1800/1900/UMTS penta-band operation. Design considerations and experimental results of the very-small-size folded loop antenna with the band-stop matching circuit are presented. © 2009 Wiley Periodicals, Inc. *Microwave Opt Technol Lett* 51: 808–814, 2009; Published online in Wiley InterScience (www.interscience.wiley.com). DOI 10.1002/mop.24147

Key words: internal mobile phone antennas; loop antennas; WWAN operation; penta-band operation; band-stop matching circuit

1. INTRODUCTION

In recent studies, the loop antennas have been shown to be very promising for application in the mobile phone as internal multi-band antennas for WWAN communications [1–8]. These multi-band loop antennas cover several or all operating bands of the GSM850 (824–894 MHz), GSM900 (890–960 MHz), GSM1800 (1710–1880 MHz), GSM1900 (1850–1990 MHz), and UMTS (1920–2170 MHz) systems [9]. With multiband operation obtained, these loop antennas occupy reasonable volume or at least 1 cm^3 inside the mobile phone. However, it is a trend for modern mobile phones that the occupied volume of the internal antenna should be decreased, with multiband operation especially penta-band operation still desirable. With decreasing volume for the internal antenna, however, it is usually a big challenge to achieve penta-band operation, especially for covering both GSM850 and GSM900 operation in the antenna's lower band.

In this study, we present a very-small-size folded loop antenna occupying 0.6 cm^3 only and yet capable of multiband operation in the mobile phone. The folded loop antenna is formed by folding a half-wavelength loop strip onto a foam base of size 0.6 cm^3 and has a similar structure as that studied in [8]; however, the antenna volume is greatly decreased from 1 to 0.6 cm^3 and still can perform GSM850/1800/1900/UMTS quad-band operation. By incorporating the antenna with a novel band-stop matching circuit of central frequency at about 1 GHz and 3-dB band-stop bandwidth of less than about 200 MHz, an additional resonance in the 900 MHz band to cover GSM900 operation can be obtained.

The adding of external matching circuits for bandwidth enhancement of the internal antenna in the mobile phone has been demonstrated [10–14]. The matching circuit studied in [10] for the internal mobile phone antennas can double the bandwidth at the

desired band; however, it also decreases the bandwidth and radiation efficiency at the other band. In [11], the matching circuit is applied to the single-band mobile phone antenna and it can also lead to the bandwidth widening at the desired band. A high-pass matching circuit in [12] is applied to the internal antenna for improving the impedance matching over the 900 MHz band, and GSM900/1800/1900/UMTS quad-band operation is obtained for the antenna. In [13], two matching circuits are added to the internal antenna having two nonresonant coupling elements, respectively, for 900 and 1800 MHz bands to achieve GSM850/900/1800/1900 quad-band operation. A matching circuit comprising a high-pass circuit and a low-pass circuit has also been applied to two resonant elements-based internal antennas for achieving GSM900/1800/1900 operation [14].

For the band-stop matching circuit studied here, it has a band-stop property and is different from the matching circuits reported in [10–14]. The studied band-stop matching circuit is a three-element circuit, also different from the conventional two-element band-stop circuit [15, 16]. This three-element band-stop matching circuit can result in an additional zero reactance in the 900 MHz band of the folded loop antenna; in this case, an additional resonance can be generated. This behavior leads to a dual-resonance excitation in the 900 MHz band for the antenna. Hence, a much widened operating band for covering GSM850/900 operation for the antenna can be achieved. Further, the proposed three-element matching circuit shows a smaller 3-dB band-stop bandwidth than the conventional two-element one. This property makes the three-element matching circuit have very small effects on the upper band of the antenna; this makes it easy for the folded loop antenna to achieve GSM850/900/1800/1900/UMTS penta-band operation by incorporating the proposed band-stop matching circuit. Results of the folded loop antenna with the three-element band-stop matching circuit are presented and discussed. Detailed effects of the proposed matching circuit on the bandwidth enhancement of the folded loop antenna are also studied.

2 PROPOSED ANTENNA WITH THE BAND-STOP MATCHING CIRCUIT

Figure 1(a) shows the geometry of the folded loop antenna with the band-stop matching circuit in the mobile phone. Detailed dimensions of the antenna in its unfolded structure are shown in Figure 1(b), and the matching circuit is given in Figure 1(c). As shown in Figure 1(a), a ground plane of size $100 \times 40 \text{ mm}^2$ is printed on the back side of a 0.8-mm thick FR4 substrate, which is treated as the system circuit board of the mobile phone. For the FR4 substrate, it is 40 mm in width and 103 mm in length, and there is a no-ground region of $3 \times 40 \text{ mm}^2$ at the top edge of the substrate for accommodating the folded loop antenna. Also note that the mobile phone studied here is covered by a 1-mm thick plastic housing of relative permittivity (ϵ_r) 3 and conductivity (σ) 0.01 S/m [see the dashed line in Fig. 1(a)] in order to simulate the housing of practical mobile phones.

The antenna is constructed by folding a 0.5-mm wide metal strip onto a foam base (not shown in the figure) of size $40 \times 5 \times 3 \text{ mm}^3$ or 0.6 cm^3 only. The folded loop is arranged to be symmetric with respect to the central line of the system circuit board. One end (point D) of the folded loop is short-circuited to the ground plane, and the other end (point B) is the antenna's feeding point. These two ends are both near the central line of the system circuit board and are separated by a small distance of 1 mm in this design. There is also a 0.5-mm gap on the front side of the circuit board between the folded loop and the top edge of the ground plane. The total length of the metal strip is about 183 mm, which is about 0.5 wavelength of 850 MHz. That is, the antenna can

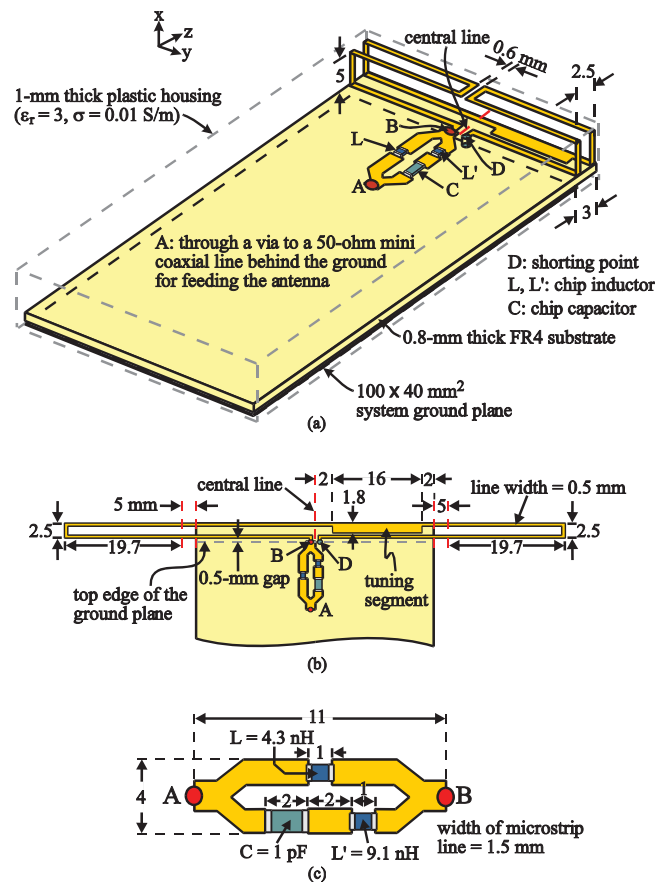


Figure 1 (a) Geometry of the folded loop antenna with the band-stop matching circuit in the mobile phone. (b) Dimensions of the antenna in its unfolded structure. (c) Layout of the matching circuit. [Color figure can be viewed in the online issue, which is available at www.interscience.wiley.com]

generate a 0.5-wavelength resonant mode at frequencies slightly lower than 900 MHz, allowing the antenna to cover GSM850 operation. On the other hand, the 1.0- and 1.5-wavelength resonant modes of the folded loop antenna can be adjusted to form a very wide operating band as the antenna's upper band to cover GSM1800/1900/UMTS operation. This adjustment is achieved by adding a tuning segment of 16 mm in length and 1.3 mm in width to the folded loop at proper location [see Fig. 1(b), the tuning segment is 2 mm away from the central line of the folded loop] to improve the impedance matching of the excited 1.0- and 1.5-wavelength resonant modes. The technique of applying this tuning segment has been studied in [8].

The matching circuit is placed between point B and point A. The matching circuit occupies an area of $4 \times 11 \text{ mm}^2$ and comprises 50- Ω microstripline sections and three lump elements which are one chip capacitor and two chip inductors. Point B of the matching circuit is connected to the folded loop antenna, and point A is connected through a via to a 50- Ω mini coaxial line behind the ground plane for feeding the antenna. All the 50- Ω microstripline sections in the two branches shown in Figure 1(c) are all 1.5 mm in width. One branch is for placing inductor L (4.3 nH in this study), whereas the other branch is for placing capacitor C (1 pF) and inductor L' (9.1 nH) in series. With this arrangement, the matching circuit shows a band-stop property with a central frequency at about 1.05 GHz and a 3-dB band-stop bandwidth of about 170 MHz only. This band-stop property helps generate an

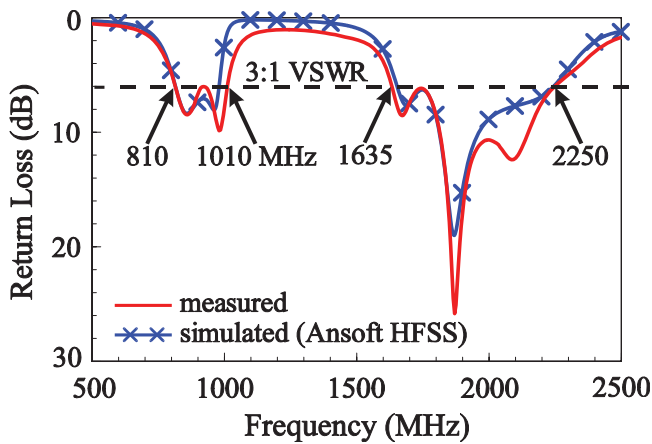


Figure 2 Measured and simulated return loss for the antenna with the matching circuit. [Color figure can be viewed in the online issue, which is available at www.interscience.wiley.com]

additional resonance at about 1 GHz with very slightly affecting the antenna's 0.5-wavelength resonant mode at about 850 MHz and the antenna's wide upper band. Penta-band operation covering GSM850/900/1800/1900/UMTS is hence obtained. Detailed effects of the three-element band-stop matching circuit on the impedance matching of the folded loop antenna are studied with the aid of Figures 5–8 in the next section.

3. RESULTS AND DISCUSSION

3.1. Antenna with the Matching Circuit

On the basis of the design dimensions given in Figure 1, the folded loop antenna with the matching circuit was constructed and tested. Figure 2 shows the measured and simulated (Ansoft HFSS [17]) return loss. Two wide operating bands for the antenna's lower and upper bands are generated with good impedance matching. Good agreement between the measured and simulated results is also seen. The lower band ranges from 810 to 1010 MHz (200 MHz in bandwidth) and the upper band covers from 1635 to 2250 MHz (615 MHz in bandwidth). The bandwidth is defined by 3:1 VSWR (6-dB return loss), which is widely accepted for internal mobile phone antenna design. Note that the lower band shows a dual-resonance behavior; the first mode is the 0.5-wavelength resonant mode of the folded loop antenna, while the second one is contributed owing to the presence of the matching circuit. This can be seen more clearly from the comparison of the simulated return loss for the antenna with and without the matching circuit shown in Figure 3. For the upper band, it is mainly formed by the antenna's 1.0- and 1.5-wavelength resonant modes (see the marked curve for the case without the matching circuit in Fig. 3); the study on the related effects can be found in [8]. With the matching circuit, there is generally no degradation effect on the impedance matching over the upper band. The two resonant modes in the upper band are slightly shifted to lower frequencies, and moreover, there are some improvements on the impedance matching of the higher frequencies around 2.1 GHz of the second resonant mode (1.5-wavelength mode) in the upper band. This leads to further improvements in the bandwidth of the upper band.

Figure 4(a) shows the simulated input impedance for the antenna with and without the matching circuit. The equivalent impedance of the matching circuit is shown in Figure 4(b), in which it is seen that the matching circuit shows a good band-stop property with a central frequency at about 1.05 GHz. The matching circuit contributes some inductance at about 1 GHz for the an-

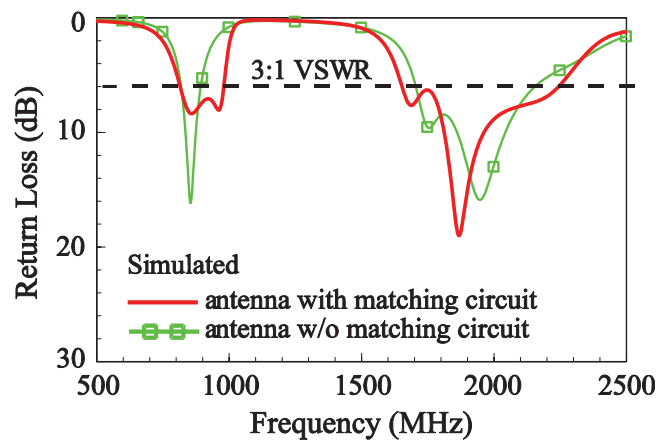
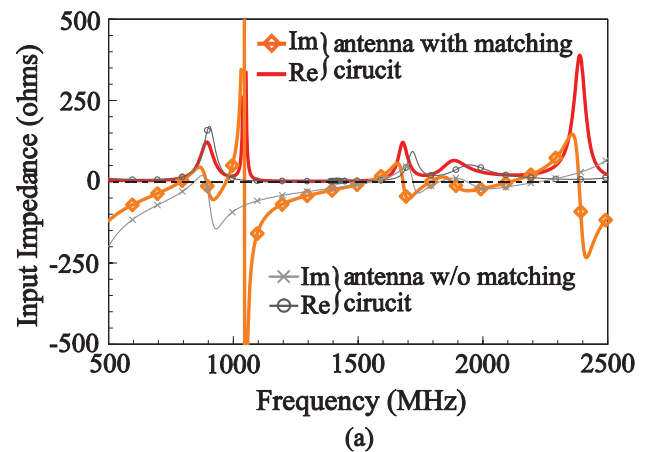
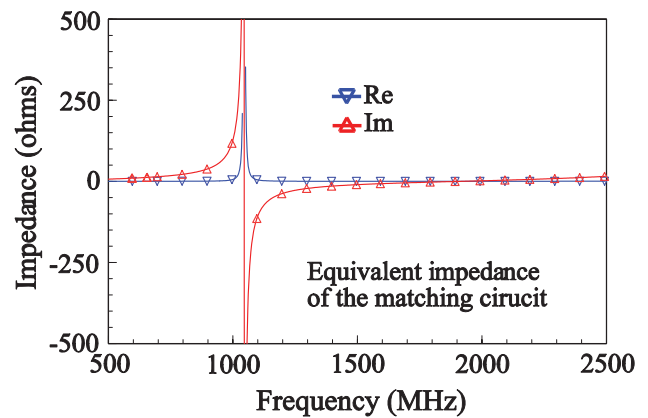


Figure 3 Simulated return loss for the proposed antenna with and without the matching circuit. [Color figure can be viewed in the online issue, which is available at www.interscience.wiley.com]

tenna; this compensates for the large input capacitance of the antenna around 1 GHz [see the curve with cross marks in Fig. 4(a)]. An additional resonance (zero reactance) at about 970 MHz [seen in Fig. 4(a)] is hence obtained, with the original 0.5-wavelength mode slightly affected. This leads to a dual-resonance



(a)



(b)

Figure 4 (a) Simulated input impedance for the antenna with and without the matching circuit. (b) Simulated equivalent impedance of the matching circuit. [Color figure can be viewed in the online issue, which is available at www.interscience.wiley.com]

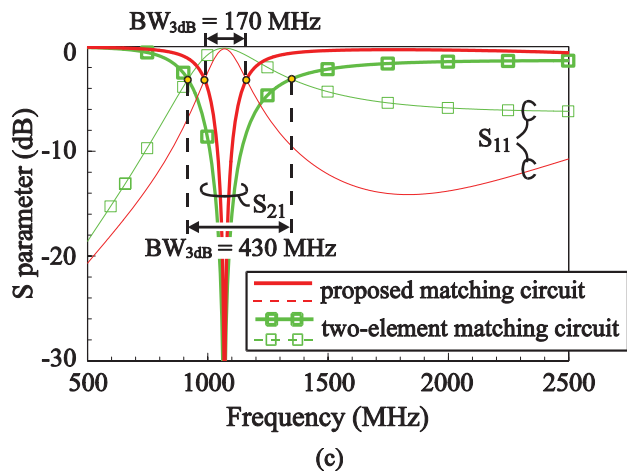
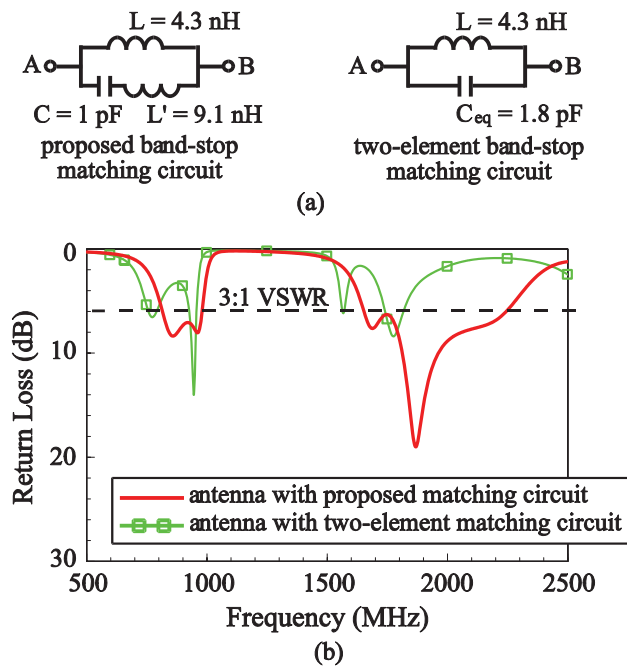


Figure 5 (a) The proposed three-element band-stop matching circuit and the two-element matching circuit. (b) Simulated return loss for the antenna with the proposed band-stop matching circuit or the two-element band-stop matching circuit. (c) Simulated S parameters of the two matching circuits in (a). [Color figure can be viewed in the online issue, which is available at www.interscience.wiley.com]

excitation for the antenna's lower band, allowing it to cover GSM850/900 operation. For frequencies over the antenna's upper band, it is seen that the equivalent impedance of the matching circuit is very small, causing relatively small effects on the impedance matching over the upper band. However, as seen in Figure 4(a), the two resonant modes in the upper band are slightly shifted to lower frequencies, and there is also a zero reactance occurred at about 2.1 GHz. The former shifts the lower-edge frequency with 3:1 VSWR of the upper band to lower frequencies, while the latter moves the upper-edge frequency with 3:1 VSWR to higher frequencies. Hence, a wider bandwidth for the antenna's upper band is obtained as discussed in Figure 3. More detailed effects of the proposed band-stop matching circuit are discussed below.

3.2. Effects of the Three-Element Band-Stop Matching Circuit

Figure 5(a) shows the equivalent circuits of the proposed three-

element band-stop matching circuit and the conventional two-element band-stop matching circuit [15, 16]. The capacitor C_{eq} in the two-element circuit is selected to be 1.8 pF, which makes the central band-stop frequency occur at about 1.05 GHz, the same as that of the three-element circuit studied here. The central frequency of the three-element circuit is derived to be Eq. (1), while that of the two-element circuit is determined by Eq. (2):

$$f_c = \frac{1}{2\sqrt{2}\pi} \sqrt{\left(\frac{L+L'}{LL'C_m} + \frac{1}{L'C}\right) - \sqrt{\left(\frac{L+L'}{LL'C_m} + \frac{1}{L'C}\right)^2 - \frac{4}{LL'CC_m}}} \quad (1)$$

$$f_c = \frac{1}{2\pi\sqrt{L(C_{eq} + C_m)}} \quad (2)$$

Note that, in the above equations, C_m is the equivalent capacitance between the microstripline sections and the ground plane, which is determined to be 3.3 pF using Ansoft HFSS. The capacitance C_m should be considered in calculating the central band-stop frequency of the matching circuit. From calculating Eqs. (1) and (2),

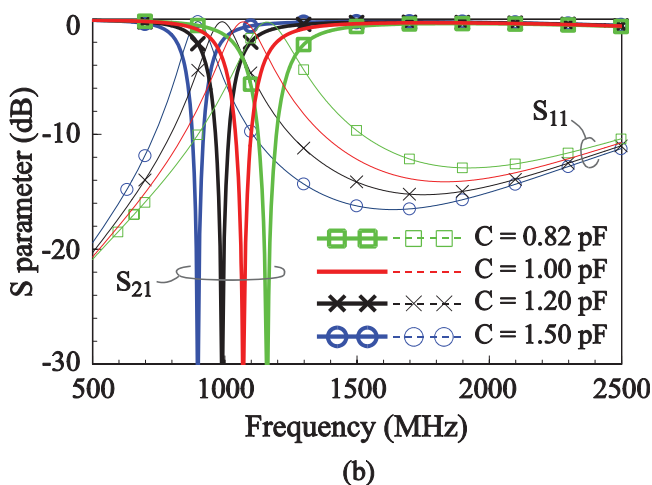
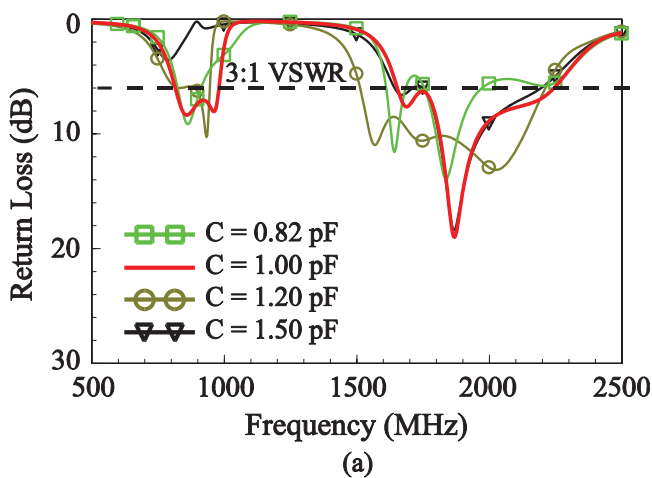


Figure 6 Simulated results of (a) the return loss for the antenna with the proposed matching circuit and (b) S parameters of the proposed matching circuit; C is varied from 0.82 to 1.50 pF. Other parameters are the same as studied in Figure 2. [Color figure can be viewed in the online issue, which is available at www.interscience.wiley.com]

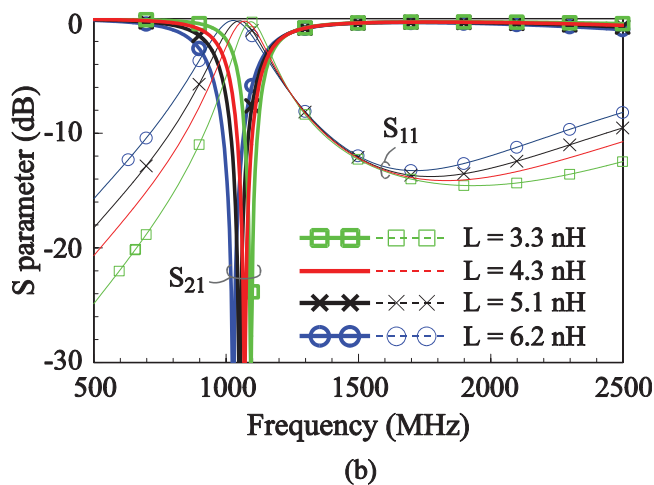
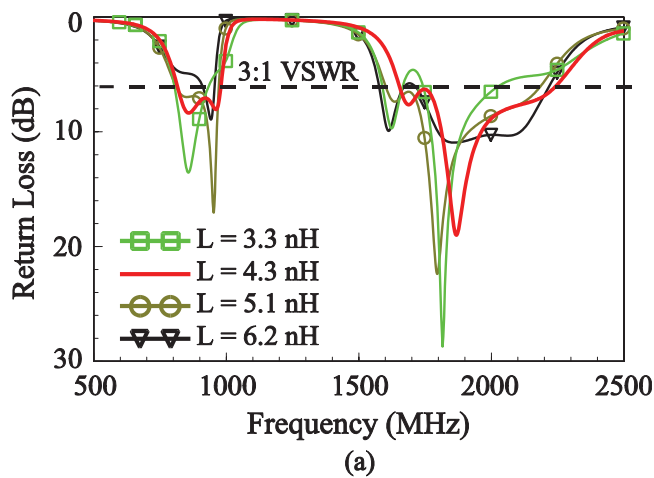


Figure 7 Simulated results of (a) the return loss for the antenna with the proposed matching circuit and (b) S parameters of the proposed matching circuit; L is varied from 3.3 to 6.2 nH. Other parameters are the same as studied in Figure 2. [Color figure can be viewed in the online issue, which is available at www.interscience.wiley.com]

the central frequencies of the three-element and two-element circuits are about the same, both at about 1.05 GHz.

Figure 6(b) shows the comparison of the simulated return loss for the antenna with the three-element circuit or the two-element circuit. It is seen that the impedance matching over the upper band is greatly affected for the case with the two-element circuit. This behavior can be explained by the simulated S parameters of the two matching circuits shown in Figure 6(c), in which the 3-dB bandwidth of the stop band of the two-element circuit is 430 MHz, much larger than that (170 MHz) of the proposed three-element circuit. This characteristic suggests that the two-element circuit will cause large effects on the impedance matching over the existing resonant modes of the folded loop antenna. On the other hand, with the use of the three-element circuit, relatively small effects on the impedance matching over the existing resonant modes, especially those in the upper band, of the folded loop antenna can be obtained.

A parametric study for varying the inductance and capacitance in the three-element circuit on the impedance matching of the folded loop antenna and on the S parameters of the matching circuit are plotted in Figures 6–8. Figure 6 shows the results for the capacitance C varied from 0.82 to 1.50 pF. It is seen that when

C is not properly chosen ($C = 1.0$ pF is selected in this study), the central band-stop frequency is shifted away from about the desired 1.05 GHz [see Fig. 6(b)], and there will be larger effects on the existing resonant modes of the folded loop antenna [see Fig. 6(a)].

Figure 7 shows the results for the inductance L varied from 3.3 to 6.2 nH. It is seen in Figure 7(a) that both the lower and upper bands are affected relatively slightly. The S parameter of the matching circuit shown in Figure 7(b) also indicates that the inductance L has small effects on the central band-stop frequency. Figure 8 shows the results for the inductance L' varied from 8.2 to 12 nH. It is seen in Figure 8(b) that the central band-stop frequency decreases when L' increases, and furthermore, the 3-dB bandwidth of the stop band also decreases. This behavior confirms the adding of the inductance L' in the proposed three-element circuit for effectively decreasing the 3-dB bandwidth of the stop band. In this case, with an additional resonance generated in the antenna's lower band, small effects on the existing resonant modes of the folded loop antenna can also be obtained.

3.3. Radiation Characteristics

Figures 9 and 10 plot the measured radiation patterns at 859, 925, 1795, 1920, and 2045 MHz (center frequencies of GSM850,

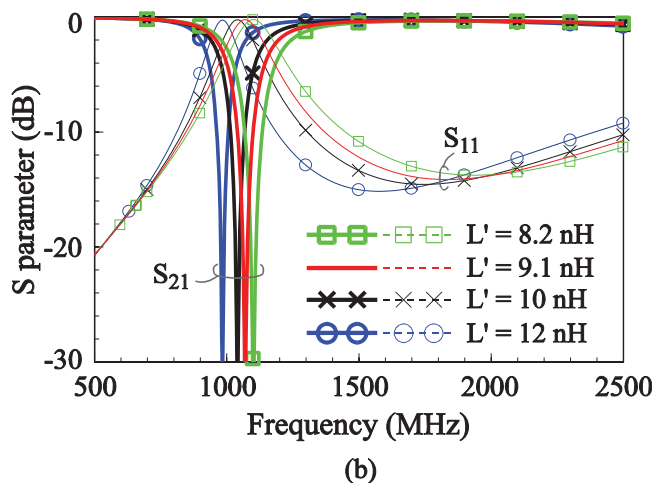
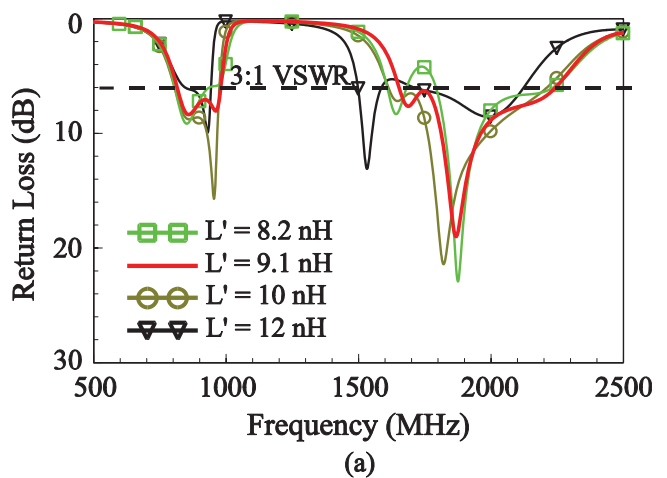


Figure 8 Simulated results of (a) the return loss for the antenna with the proposed matching circuit and (b) S parameters of the proposed matching circuit; L' is varied from 8.2 to 12 nH. Other parameters are the same as studied in Figure 2. [Color figure can be viewed in the online issue, which is available at www.interscience.wiley.com]

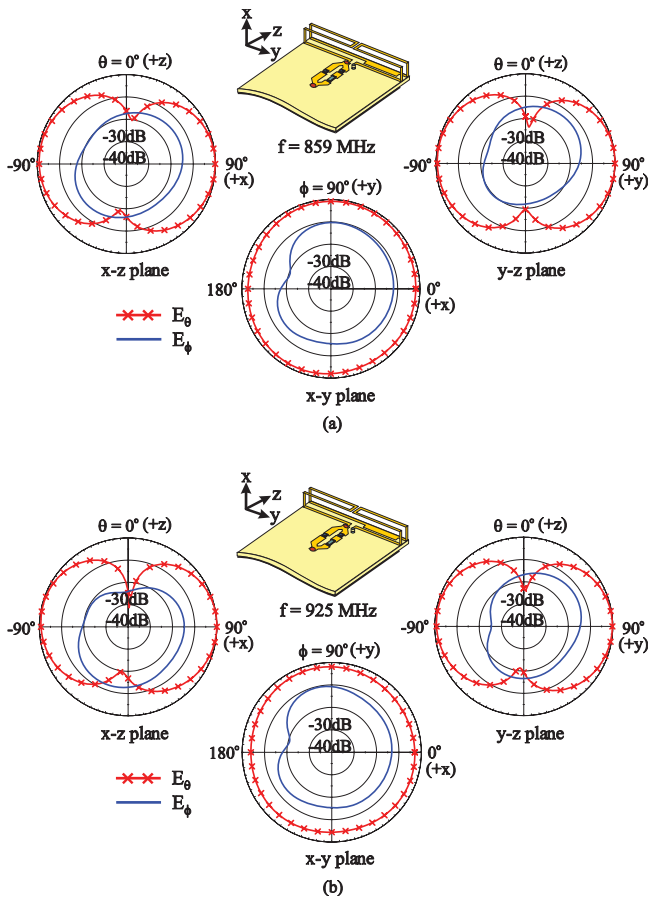


Figure 9 Measured radiation patterns at (a) 859 MHz and (b) 925 MHz for the antenna studied in Figure 2. [Color figure can be viewed in the online issue, which is available at www.interscience.wiley.com]

GSM900, GSM1800, GSM1900, UMTS bands). The radiation patterns at 859 and 960 MHz show monopole-like radiation patterns, and omnidirectional radiation in the azimuthal plane (x - y plane) is generally observed. For the radiation patterns at 1795, 1920, and 2045 MHz, more variations in the patterns are seen. These measured patterns are in general similar to those observed for the conventional internal mobile phone antennas [9]. Figure 11 presents the measured antenna gain and simulated radiation efficiency. For frequencies over the GSM850/900 band, the antenna gain is about -1.0 to 0.1 dBi, while that for the GSM1800/1900/UMTS band ranges from about 1.3 – 2.6 dBi. For the radiation efficiency over the GSM850/900 band, it is about 50 – 63% , while that for the GSM1800/1900/UMTS band varies from about 50 – 83% .

4. CONCLUSION

An internal penta-band folded loop antenna with a band-stop matching circuit suitable for mobile phone application has been proposed. The folded loop antenna is configured to occupy a very small volume of $40 \times 5 \times 3 \text{ mm}^3$ or 0.6 cm^3 only and is incorporated with a three-element band-stop matching circuit. The folded loop antenna itself can generate its 0.5 -, 1.0 -, and 1.5 -wavelength modes for covering GSM850/1800/1900/UMTS operation. With the presence of the matching circuit, an additional

resonance in the 900 MHz band can be generated for covering GSM900 operation, with very slightly affecting the existing resonant modes of the folded loop antenna. This makes the proposed design to successfully cover GSM850/900/1800/1900/UMTS penta-band operation. A parametric study on the detailed effects of the proposed three-element band-stop matching has also been presented. Good radiation characteristics for frequencies over the five operating bands for WWAN communication have also been obtained.

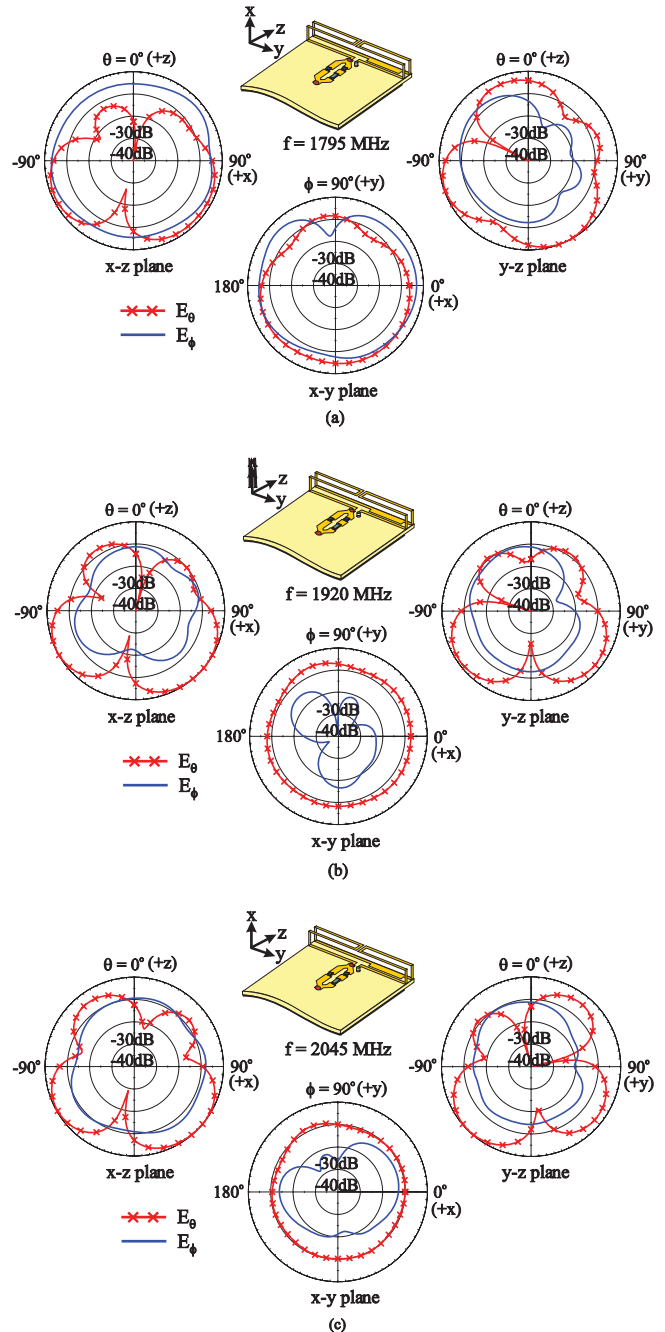


Figure 10 Measured radiation patterns at (a) 1795 MHz, (b) 1920 MHz, and (c) 2045 MHz for the antenna studied in Figure 2. [Color figure can be viewed in the online issue, which is available at www.interscience.wiley.com]

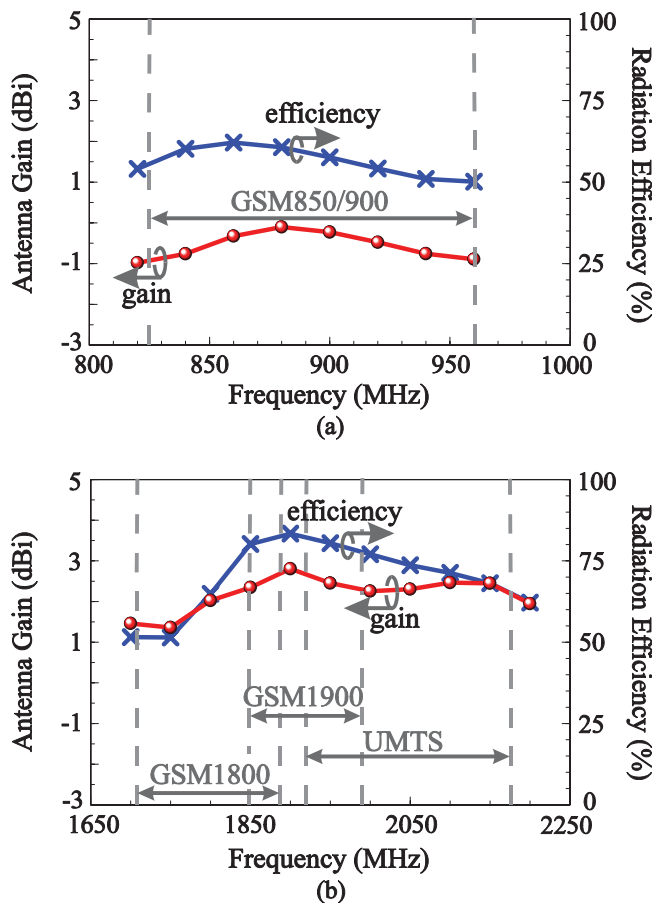


Figure 11 Measured antenna gain and radiation efficiency for the antenna studied in Figure 2. (a) The GSM850/900 band. (b) The GSM1800/1900/UMTS band. [Color figure can be viewed in the online issue, which is available at www.interscience.wiley.com]

REFERENCES

1. B.K. Yu, B. Jung, H.J. Lee, F.J. Harackiewicz, and B. Lee, A folded and bent internal loop antenna for GSM/DCS/PCS operation of mobile handset applications, *Microwave Opt Technol Lett* 48 (2006), 463–467.
2. B. Jung, H. Rhyu, Y.J. Lee, F.J. Harackiewicz, M.J. Park, and B. Lee, Internal folded loop antenna with tuning notches for GSM/GPS/DCS/PCS mobile handset applications, *Microwave Opt Technol Lett* 48 (2006), 1501–1504.
3. C.I. Lin and K.L. Wong, Internal meandered loop antenna for GSM/DCS/PCS multiband operation in a mobile phone with the user's hand, *Microwave Opt Technol Lett* 49 (2007), 759–765.
4. Y.W. Chi and K.L. Wong, Internal compact dual-band printed loop antenna for mobile phone application, *IEEE Trans Antennas Propagat* 55 (2007), 1457–1462.
5. W.Y. Li and K.L. Wong, Surface-mount loop antenna for AMPS/GSM/DCS/PCS operation in the PDA phone, *Microwave Opt Technol Lett* 49 (2007), 2250–2254.
6. C.H. Wu and K.L. Wong, Internal hybrid loop/monopole slot antenna for quad-band operation in the mobile phone, *Microwave Opt Technol Lett* 50 (2008), 795–801.
7. C.I. Lin and K.L. Wong, Internal multiband loop antenna for GSM/DCS/PCS/UMTS operation in the small-size mobile phone, *Microwave Opt Technol Lett* 50 (2008), 1279–1285.
8. Y.W. Chi and K.L. Wong, Small-Size Multiband Folded Loop Antenna for Small-Size Mobile Phone, *IEEE Antennas Propagat Int Symp Dig*, San Diego, CA, 2008, Oral Session 313.
9. K.L. Wong, *Planar antennas for wireless communications*, Wiley, New York, 2003.

10. J. Ollikainen, O. Kivekas, C. Icheln, and P. Vainikainen, Internal multiband handset antenna realized with an integrated matching circuit, in *Proceedings of 12th International Conference Antennas Propagat* Vol. 2, (2003), pp. 629–632.
11. T. Ranta, Dual-resonant antenna, U.S. Patent No. US 7,242,364 (2007).
12. M. Tzortzakakis and R.J. Langley, Quad-band internal mobile phone antenna, *IEEE Trans Antennas Propagat* 55 (2007), 2097–2103.
13. J. Villanen, C. Icheln, and P. Vainikainen, A coupling element-based quad-band antenna element structure for mobile terminals, *Microwave Opt Technol Lett* 49 (2007), 1277–1282.
14. T. Oshiyama, H. Mizuno and Y. Suzuki, Multi-band antenna, U.S. Patent Publication No. US 2007/0249313 (2007).
15. D.M. Pozar, *Microwave engineering*, Wiley, New York, 1998.
16. R. Ludwig and P. Bretchko, *RF circuit design theory and applications*, Prentice-Hall, New Jersey, 2000.
17. Ansoft Corporation, Available at <http://www.ansoft.com/products/hf/hfss/>, Ansoft Corporation HFSS.

© 2009 Wiley Periodicals, Inc.

DESIGN OF AN ULTRA-WIDEBAND ANTENNA WITH A NOVEL DUAL BAND-NOTCHED STRUCTURE

J. Ma, Y.-Z. Yin, J.-Y. Deng, and Q. Ma

National Key Laboratory of Antenna and Microwave Technology, Xidian University, Xi'an, Shaanxi, People's Republic of China; Corresponding author: majie_xidian@163.com

Received 16 July 2008

ABSTRACT: A novel dual band-notched monopole ultra-wideband antenna is proposed, in which the parasitic strip creates one band-notch at 5.5 GHz and the tuning stub produces another band-notch at 3.5 GHz. The experimental results show that the proposed antenna, with a compact size of $20 \times 31.5 \text{ mm}^2$, has a bandwidth of 3.1–10.6 GHz with voltage standing wave ratio (VSWR) less than 2, except the bandwidths of 3.3–3.7 GHz for WIMAX and 5.15–5.825 GHz for WLAN. By changing the lengths of the parasitic strip and the tuning stub, the central frequencies of the dual notched bands can be adjusted easily. In addition, there is a little influence on a band-notched characteristic when another is changed. © 2009 Wiley Periodicals, Inc. *Microwave Opt Technol Lett* 51: 814–817, 2009; Published online in Wiley InterScience (www.interscience.wiley.com). DOI 10.1002/mop.24163

Key words: ultra-wideband; parasitic strip; tuning stub; dual band-notched

1. INTRODUCTION

With the development of modern wireless and mobile communication, the ultra-wideband systems have attracted much attention recently because of its great advantages including high speed data rate, small size, and low power consumption. However, according to IEEE 802.11a, HIPERLAN/2, and IEEE 802.16, some narrow bands, such as WLAN systems (5.15–5.825 GHz) and WIMAX systems (3.3–3.7 GHz), exist during the bandwidth of ultra-wideband (3.1–10.6 GHz). Therefore, to avoid EM interferences between these systems and UWB communication systems, a band elimination characteristic is necessary in UWB antennas. Recently, several UWB antennas with frequency band-rejection function have been reported [1–6]. But, most of the proposed antennas only have one band-notched characteristics [1–3]. Two UWB antennas with dual band stops have recently been proposed [4, 5]. The dual band stops are formed by cutting two or three U-shaped or C-